Inorg. Chem. **2005**, *44*, 6248–6255

Coordination of Nitroxide and Nitronyl-nitroxide Organic Radicals to Trimeric Perfluoro-*o*-phenylene Mercury

Mason R. Haneline and François P. Gabbaï*

Texas A&M University, Chemistry TAMU 3255, College Station, Texas 77843-3255

Received April 6, 2005

The interaction of trimeric perfluoro-*o*-phenylene mercury (**1**) with TEMPO (1,1,5,5-tetramethylpentamethylene nitroxide) in CH_2Cl_2 leads to the formation of the 1:1 adduct [**1**•TEMPO] (**2**). The same reaction carried out with NIT-Ph (2-(phenyl)-4,4,5,5-tetramethylimidazoline-1-oxyl-3-oxide) leads to the formation of either [**1**•NIT-Ph•**1**] (**3**) or [**1**•NIT-Ph]$_n$ (**4**), depending on the amount of NIT-Ph present in solution. Adducts **2**, **3**, and **4** have been fully characterized and their crystal structures determined. The solid-state structure of **2** contains molecules of [**1**•TEMPO] in which the nitroxide oxygen atom is triply coordinated to the mercury centers of **1**. A similar situation is encountered in the structure of **3** where each oxygen atom of the NIT-Ph molecule interacts with the mercury centers of an adjacent molecule of **1**. The structure of **4** consists of extended helical polymeric chains that contain alternating molecules of **1** and NIT-Ph. As in **2** and **3**, the interactions responsible for the formation of these chains involve the triple coordination of the oxygen atoms of the NIT-Ph molecule to the mercury centers of **1**. DFT calculations suggest that the bonding in adducts such as **2**, **3**, and **4** is most likely dominated by electrostatic rather than covalent interactions. In agreement with this view, magnetic susceptibility measurements carried out on these adducts indicate that **1** does not mediate significant coupling between organic radicals coordinated on either side of the trinuclear core.

Introduction

Polyfunctional organomercurials featuring proximal metal centers have been extensively studied as polydentate Lewis acids. Typical examples of such complexes include 1,8-bis-(mercurio)naphathalenes,[1] 1,2-bis(mercurio)benzenes,[2] and various macrocyclic[3,4] species such as mercuracarborands.[5] Such derivatives have been investigated for the multiple electrophilic complexation of both anionic and neutral electron-rich substrates. Perfluoro-*o*-phenylene mercury (**1**) is a prototypical example of such polyfunctional Lewis acids.[3,4] It exhibits a fascinating coordination chemistry with anions and has been employed in the formation of hexa-coordinated halide complexes.[6] This trinuclear complex also interacts with neutral electron-rich substrates[7] including organic carbonyls,[8−10] nitriles,[11] and sulfoxides[12] to form

* E-mail: gabbai@mail.chem.tamu.edu.

(1) Schmidbaur, H.; Öller, H.-J.; Wilkinson, D. L.; Huber, B. *Chem. Ber.* **1989**, *122*, 31−36.

(2) (a) Beauchamp, A. L.; Olivier, M. J.; Wuest, J. D.; Zacharie, B. *Organometallics* **1987**, *6*, 153−156. (b) Tschinkl, M.; Schier, A.; Riede, J.; Gabbaï, F. P. *Organometallics* **1999**, *18*, 1747−1753. (c) Vaugeois, J.; Wuest, J. D. *J. Am. Chem. Soc.* **1998**, *120*, 13016−13022. (d) Vaugeois, J.; Simard, M.; Wuest, J. D. *Organometallics* **1998**, *17*, 1215−1219. (e) Simard, M.; Vaugeois, J.; Wuest, J. D. *J. Am. Chem. Soc.* **1993**, *115*, 370−372. (f) Wuest, J. D.; Zacharie, B. *J. Am. Chem. Soc.* **1987**, *109*, 4714−4715. (g) Beauchamp, A. L.; Olivier, M. J.; Wuest, J. D.; Zacharie, B. *J. Am. Chem. Soc.* **1986**, *108*, 73−77. (h) Wuest, J. D.; Zacharie, B. *J. Am. Chem. Soc.* **1985**, *107*, 6121−6123. (i) Wuest, J. D.; Zacharie, B. *Organometallics* **1985**, *4*, 410−411.

(3) Shur, V. B.; Tikhonova, I. A. *Russ. Chem. Bull.* **2003**, *52*, 2539−2554.

(4) Haneline, M. R.; Taylor, R.; Gabbaï, F. P. *Chem. Eur. J.* **2003**, *9*, 5188−5193.

(5) (a) Hawthorne, M. F.; Zheng, Z. *Acc. Chem. Res.* **1997**, *30*, 267−276. (b) Wedge, T. J.; Hawthorne, M. F. *Coord. Chem. Rev.* **2003**, *240* (1−2), 111−128.

(6) (a) Chistyakov, A. K.; Stankevich, I. V.; Gambaryan, N. P.; Struchkov, Y. T.; Yanovsky, A. I.; Tikhonova, I. A.; Shur, V. B. *J. Organomet. Chem.* **1997**, *536*, 413−424. (b) Shur, V. B.; Tikhonova, I. A.; Yanovskii, A. I.; Struchkov, Y. T.; Petrovskii, P. V.; Panov, S. Y.; Furin, G. G.; Vol'pin, M. E. *J. Organomet. Chem.* **1991**, *418*, C29−C32. (c) Shur, V. B.; Tikhonova, I. A.; Yanovskii, A. I.; Struchkov, Y. T.; Petrovskii, P. V.; Panov, S. Y.; Furin, G. G.; Vol'pin, M. E. *Dokl. Akad. Nauk. SSR* **1991**, *321*, 1002−1004. (d) Shur, V. B.; Tikhonova, I. A.; Dolgushin, F. M.; Yanovsky, A. I.; Struchkov, Y. T.; Volkonsky, A. Y.; Solodova, E. A.; Panov, S. Y.; Petrovskii, P. V.; Vol'pin, M. E. *J. Organomet. Chem.* **1993**, *443*, C19−C21. (e) Koomen, J. M.; Lucas, J. E.; Haneline, M. R.; Beckwith King, J. D.; Gabbaï, F.; Russell, D. H. *Int. J. Mass Spectrom.* **2003**, *225*, 225−231.

(7) Tsunoda, M.; Gabbaï, F. P. *J. Am. Chem. Soc.* **2003**, *125*, 10492−10493.

(8) Ball, M. C.; Brown, D. S.; Massey, A. G. *J. Organomet. Chem.* **1981**, *206*, 265−277.

10.1021/ic050528a CCC: $30.25
Published on Web 08/04/2005

Chart 1. Schematic Structures of **1**, the 1:1 and 1:2 Complexes Formed by **1,** and Electron-Rich Substrates (L)

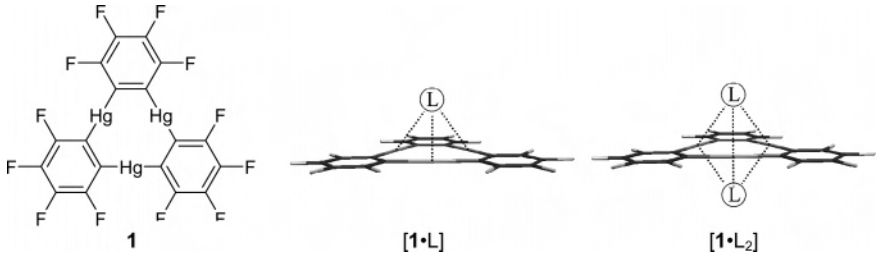

Chart 2

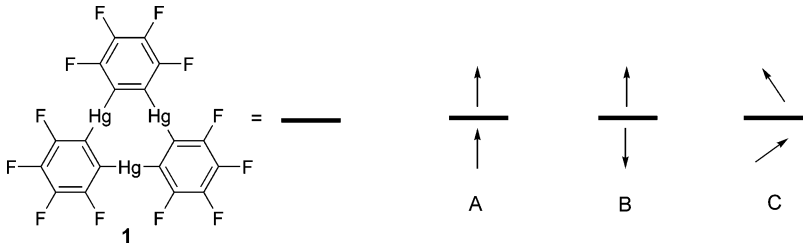

discrete [**1**•L] and [**1**•L_2] complexes in which the electron rich terminus of the substrates interacts simultaneously with the three mercury atoms of **1** (Chart 1). In the [**1**•L_2] complexes, two molecules of the donor are coordinated to the mercury centers of **1** on either side of the molecular plane. Work carried out in our laboratory also demonstrates that **1** is a remarkable building block for the construction of supramolecular materials.[3,4] In particular, **1** readily interacts with various arenes to form extended binary stacks in which the arene is weakly π-coordinated to the mercury centers of **1**.[13] These supramolecules feature distinct physical properties and display intense room-temperature phosphorescence of the arene as a result of a mercury heavy atom effect.[13] As part of our continuing interest in the chemistry of this molecule, we are actively exploring its potential for the elaboration of novel materials.

Nitroxides and nitronyl nitroxides are some of the most stable organic radicals.[14] Like organic carbonyls, these molecules feature an electron-rich terminal oxygen atom that should readily coordinate to the mercury centers of **1**. If 1:2 complexes are accessible, three distinct magnetic situations (A−C) can be envisioned (Chart 2). If **1** is able to mediate magnetic interactions, the organic radicals could couple in either a ferromagnetic (A) or an antiferromagnetic fashion (B). Also, it can be envisaged that **1** does not mediate magnetic interactions, leading to a situation in which the organic radicals remain uncoupled (C). To determine which of these situations occurs, we have now prepared and studied a series of adducts involving **1** and 1,1,5,5-tetramethylpentamethylene nitroxide (TEMPO) or 2-(phenyl)-4,4,5,5-tetramethylimidazoline-1-oxyl-3-oxide (NIT-Ph) nitronyl radicals.

Experimental Section

General: *Due to the toxicity of the mercury compounds discussed in these studies, extra care was taken at all times to avoid contact with solid, solution, and airborne particulate mercury compounds. All experiments were carried out in a well-aerated fume hood.* Atlantic Microlab, Inc., Norcross, GA, performed the elemental analyses. Infrared spectra were recorded as KBr pellets on a Mattson Genesis Series FTIR. NIT-Ph was synthesized according to the published procedure.[15] Commercially available starting materials and solvents were purchased from Aldrich Chemical and were used as provided. Compound **1** was prepared according to the published procedure outlined by Sartori and Golloch.[16] Magnetic susceptibility and magnetization measurements were carried out with a Quantum Design SQUID magnetometer MPMS-XL. dc magnetic measurements were performed with an applied field of 1000 G in the 2−300 K temperature range. Data were corrected for the diamagnetic contributions calculated from the Pascal constants.[17] The small discontinuity observed in the thermal variation of the X_mT product for compound **2** and **3** (Figure 6) is caused by a subtraction of the magnetization obtained for the sample holder (diamagnetic) from the magnetization obtained for the actual sample. This discontinuity is accentuated by the small size of the sample and the fact that the compounds are magnetically dilute (see MPMS Application Note 1014-213 − Quantum Design − available on the Internet at http://www.qdusa.com/).

(9) King, J. B.; Tsunoda, M.; Gabbaï, F. P. *Organometallics* **2002**, *21*, 4201−4205.
(10) King, J. B.; Haneline, M. R.; Tsunoda, M.; Gabbaï, F. P. *J. Am. Chem. Soc.* **2002**, *124*, 9350−9351.
(11) (a) Tikhonova, I. A.; Dolgushin, F. M.; Yanovsky, A. I.; Starikova, Z. A.; Petrovskii, P. V.; Furin, G. G.; Shur, V. B. *J. Organomet. Chem.* **2000**, *613*, 60−67. (b) Tikhonova, I. A.; Dolgushin, F. M.; Tugashov, K. I.; Furin, G. G.; Petrovskii, P. V.; Shur, V. B. *Russ. Chem. Bull.* **2001**, *50*, 1673−1678. (c) Tikhonova, I. A.; Dolgushin, F. M.; Tugashov, K. I.; Ellert, O. G.; Novotortsev, V. M.; Furin, G. G.; Antipin, M. Yu.; Shur, V. B. *J. Organomet. Chem.* **2004**, *689*, 82−87. (d) Baldamus, J.; Deacon, G. B.; Hey-Hawkins, E.; Junk, P. C.; Martin, C. *Aust. J. Chem.* **2002**, *55*, 195−198.
(12) Tikhonova, I. A.; Dolgushin, F. M.; Tugashov, K. I.; Petrovskii, P. V.; Furin, G. G.; Shur, V. B. *J. Organomet. Chem.* **2002**, *654*, 123−131.
(13) (a) Haneline, M. R.; Tsunoda, M.; Gabbaï, F. P *J. Am. Chem. Soc.* **2002**, *124*, 3737−3742. (b) Haneline, M. R.; King, J. B.; Gabbaï, F. P. *J. Chem. Soc., Dalton Trans.* **2003**, *13*, 2686−2690. (c) Omary, M. A.; Kassab, R. M.; Haneline M. R.; Elbjeirami, O.; Gabbaï, F. P. *Inorg. Chem.* **2003**, *42*, 2176−2178.
(14) Volodarsky, L. B.; Reznikov, V. A.; Ovcharenko, V. I. *Synthetic Chemistry of Stable Nitroxides*; CRC Press: Boca Raton, FL, 1994.
(15) Ullman, E. F.; Osiecki, J. H.; Boocock, D. G. B.; Darcy, R. *J. Am. Chem. Soc.* **1972**, *94*, 7049−7059.
(16) Sartori, P.; Golloch, A. *Chem. Ber.* **1968**, *101*, 2004−2009.
(17) *Theory and Applications of Molecular Paramagnetism*; Boudreaux, E. A., Mulay, L. N., Eds.; John Wiley & Sons: New York, 1976.

Synthesis of [1•TEMPO] (2). A solution of compound **1** (100 mg, 96 μmol) in CH_2Cl_2 was mixed with a solution of TEMPO (15 mg, 98 μmol) in CH_2Cl_2. Upon slow evaporation of the solvent, pale yellow crystals of compound **2** were observed (109 mg, yield: 95%). mp 239 °C decomposition. Anal. Calcd for $C_{27}H_{18}F_{12}Hg_3NO$: C, 27.01; H, 1.51. Found: C, 27.03; H, 1.42.

Synthesis of [1•NIT-Ph•1] (3). A solution of compound **1** (100 mg, 96 μmol) in CH_2Cl_2 was mixed with a solution of NIT-Ph (22.4 mg, 96 μmol) in CH_2Cl_2. Upon evaporation of the solvent, the crystals were washed with hexanes to remove excess NIT-Ph. The remaining pink crystals were washed quickly with 0.5 mL of CH_2Cl_2, affording 40 mg of compound **3** (yield: 36%). mp 220 °C decomposition. Anal. Calcd for $C_{49}H_{17}F_{24}Hg_6N_2O_2$: C, 25.35; H, 0.74. Found: C, 25.57; H, 0.72.

Synthesis of [1•NIT-Ph] (4). A solution of compound **1** (100 mg, 96 μmol) in CH_2Cl_2 was mixed with a solution of NIT-Ph (100 mg, 0.529 mmol) in CH_2Cl_2. Upon evaporation of the solvent, the crystals were washed with hexanes to remove excess NIT-Ph. The remaining purple crystals were washed quickly with 0.5 mL of CH_2Cl_2, affording 90 mg of compound **4** (yield: 73%). mp 190 °C decomposition. Anal. Calcd for $C_{31}H_{17}F_{12}Hg_3N_2O_2$: C, 29.10; H, 1.34. Found: C, 28.99; H, 1.32.

Single-Crystal X-ray Analysis. X-ray data for **2**−**4** were collected on a Bruker Smart-CCD diffractometer using graphite-monochromated Mo Kα radiation (λ = 0.71073 Å). Specimens of suitable size and quality were selected and mounted onto a glass fiber with Apezion grease and run at 110 K. The structures were solved by direct methods, which successfully located most of the non-hydrogen atoms. Subsequent refinement on F^2 using the SHELXTL/PC package (version 6.1) allowed location of the remaining non-hydrogen atoms.

Calculations. Geometry optimization and single-point energy calculations were performed using density functional theory (DFT) in the Amsterdam density functional package (ADF).[18−20] The Becke exchange functional and the Lee−Yang−Parr correlation functional (BLYP) were utilized in the calculation.[21,22] The triple-ζ, double-polarization (TZ2P) basis function was used. The scalar zero-order-regular-approximation (ZORA) was applied to account for relativistic effects. The cores of atoms were frozen, C and F up to the 1s level and Hg up to the 4d level. The Dirac utility was used to generate relativistic frozen core potentials for the scalar ZORA calculations. All quoted electronic structure data from optimized structures and single-point energy data use an integration of 6.0. The energy convergence criterion was set at 10^{-6} au, and the geometry was constrained to be D_3.

Results and Discussion

Combining equimolar CH_2Cl_2 solutions of **1** and TEMPO affords pale yellow crystals of [**1**•TEMPO] (**2**) upon slow evaporation (Scheme 1). The same experiment carried out in the presence of excess TEMPO does not yield a 2:1 complex. When **1** and NIT-Ph are combined in an equimolar

Scheme 1

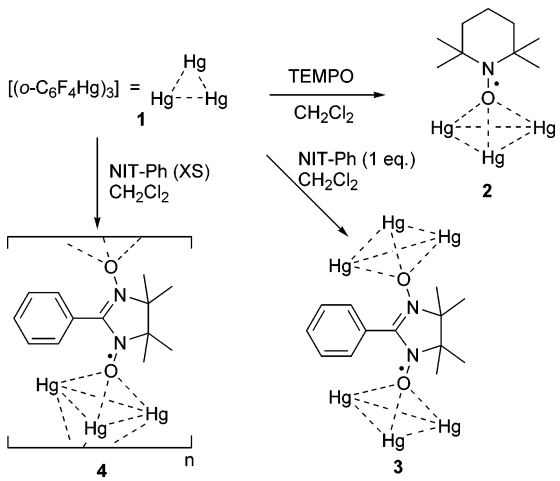

ratio in CH_2Cl_2, slow evaporation of the solvent leads to the formation of pink crystals of the 2:1 adduct [**1**•NIT-Ph•**1**] (**3**) and purple needles of the 1:1 adduct [**1**•NIT-Ph] (**4**) (Scheme 1). High yields of the latter were obtained when a large excess of NIT-Ph was employed. The composition of **2**−**4** was confirmed by elemental analysis. Each adduct was found to be air-stable and decomposed at temperatures above 190 °C. Keeping in mind that organomercurials are sometimes used to generate organic radicals, the observed stability of **1** in the presence of a radical trap such as TEMPO is noteworthy. The EPR spectra of these compounds in CH_2Cl_2 correspond to those of the free radical, suggesting dissociation of the adducts in solution. A similar conclusion was derived from NMR spectroscopic measurements for aldehyde or ketone adducts of **1** which do not subsist in solution.[9] The lability of this type of complexes points to the weakness of the bonding interactions involving **1** and organic substrates containing terminal oxo-ligands. The N−O stretching frequency in **3** (1353 cm^{-1}, KBr) and **4** (1354 cm^{-1}, KBr) is lower than that in pure NIT-Ph (1367 cm^{-1}, KBr), suggesting a moderate weakening of the N−O bond.[23] In the case of **2**, the N−O stretching vibration could not be detected because of overlap with bands from the trinuclear mercury complex.

Compound **2** crystallizes in the triclinic space group $P\bar{1}$ with one molecule of [**1**•TEMPO] in the asymmetric unit (Figure 1, Table 1). The resulting Hg−O distances range from 2.889(11) to 3.141(12) Å and are well within the sum of the van der Waals radii for mercury (r_{vdw} = 1.75 Å)[24,25] and oxygen (r_{vdw} = 1.54 Å).[26] As a result of these interactions, the oxygen atom is essentially equidistant from the three Lewis acidic sites and sits at a distance, *d*, of 2.17 Å from the plane defined by the three mercury atoms. The N−O bond of the nitroxide is nearly perpendicular to this plane and forms an angle, α, of 86.9° (Figure 1). The metrical

(18) ADF2003.01. SCM, Theoretical Chemistry, Vrije Universiteit, Amsterdam, The Netherlands.
(19) Guerra, C. F.; Snijders, J. G.; Te Velde, G.; Baerends, E. *J. Theor. Chem. Acc.* **1998**, *99*, 391−403.
(20) Te Velde, G.; Bickelhaupt, F. M.; Baerends, E. J.; Fonseca Guerra, C.; Van Gisbergen, S. J. A.; Snijders, J. G.; Ziegler, T. *J. Comput. Chem.* **2001**, *22*, 931−967.
(21) Becke, A. D. *Phys. Rev. A: At., Mol., Opt. Phys.* **1988**, *38*, 3098−3100.
(22) Lee, C.; Yang, W.; Parr, R. G. *Phys. Rev. B: Condens. Matter* **1988**, *37*, 785−789.
(23) Ullman, E. F.; Osiecki, J. H.; Boocock, D. G. B.; Darcy, R. *J. Am. Chem. Soc.* **1972**, *94*, 7049−7059.
(24) Canty, A. J.; Deacon, G. B. *Inorg. Chim. Acta* **1980**, *45*, L225−L227.
(25) Pyykkö, P.; Straka, M. *Phys. Chem. Chem. Phys.* **2000**, *2*, 2489−2493.
(26) Nyburg, S. C.; Faerman, C. H. *Acta Crystallogr., Sect. B* **1985**, *41*, 274−279.

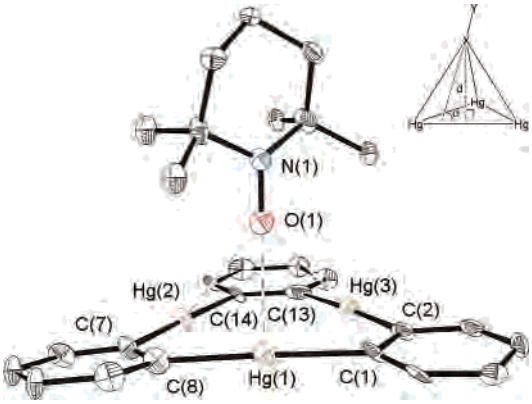

Figure 1. Compound **2** with 50% thermal ellipsoids (fluorine and hydrogen atoms omitted for clarity). Selected bond distances (Å) and angles (°): Hg(1)−O(1) 3.141(12), Hg(2)−O(1) 2.989(12), Hg(3)−O(1) 2.889(11), Hg(1)−C(1) 2.109(16), Hg(1)−C(8) 2.096(18), Hg(2)−C(7) 2.096(18), Hg(2)−C(14) 2.115(16), Hg(3)−C(2) 2.034(19), Hg(3)−C(13) 2.06(2), O(1)−N(1) 1.306(18), C(8)−Hg(1)−C(1) 175.3(7), C(7)−Hg(2)−C(14) 176.5(7), C(2)−Hg(3)−C(13) 177.1(7). The inset (top, right) shows the angle α and the distance *d* used to describe the orientation of an electron-rich functionality (X−Y) with respect to the trinuclear core of **1**.

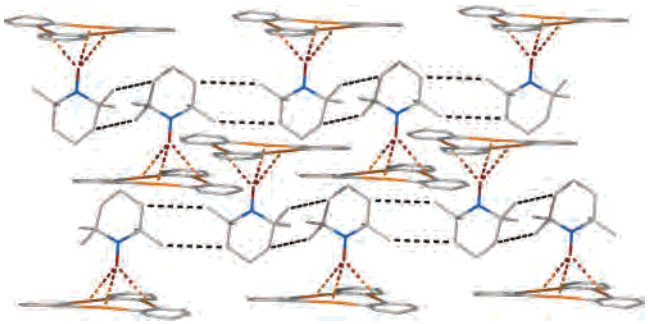

Figure 2. Extended structure of **2**. Dashed lines show short distances between the TEMPO molecules.

and angular parameters observed in **2** resemble those encountered in [**1**•acetone] (α = 85.6°, *d* = 1.945 Å, Hg−O = 2.810(12)−2.983(12) Å),[10] [**1**•acetaldehyde] (α = 66.3°, *d* = 2.086 Å, Hg−O = 2.912(13)−2.965(8) Å),[9] [**1**•$(DMF)_2$] (α = 67.7 and 88.3°, *d* = 1.990 and 2.062 Å, Hg−O = 2.799(5)−3.042(5) Å).[11,12] An examination of the extended structure of **2** reveals that the shortest intermolecular distances between neighboring TEMPO molecules do not involve the N−O functionality but instead occur between C−H groups (Figure 2). Based on the calculated position of the hydrogen atoms, these CH···HC distances can be estimated to be in the 2.5−2.7 Å range. Neighboring molecules of [**1**•TEMPO] form offset $\pi-\pi$ stacking interactions. These interactions (not pictured) occur between the phenylene ring containing C(1), its symmetry equivalent generated by $[-x+1, -y+1, -z+3]$ (centroid distance = 3.70 Å), and the phenylene ring containing C(13) in a neighboring molecule generated by $[-x+1, -y+1, -z+2]$ (centroid distance = 4.03 Å). Similar $\pi-\pi$ stacking interactions have been observed in the crystal structure of other perfluoro-*o*-phenylene mercury derivatives.[27]

(27) Tschinkl, M.; Schier, A.; Riede, J.; Gabbaï F. P. *Angew. Chem., Int. Ed.*. **1999**, *38*, 3547−3549.

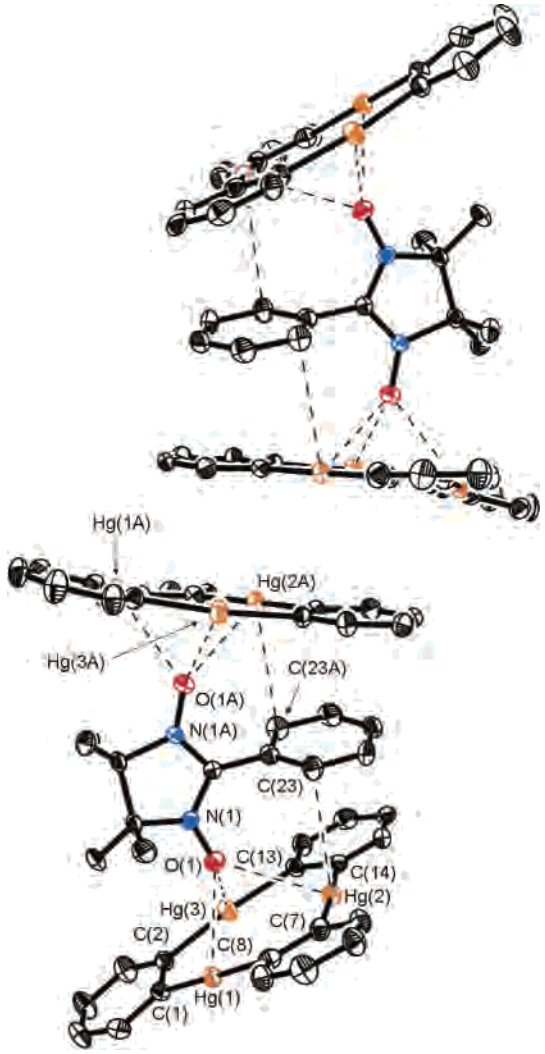

Figure 3. Compound **3** with 50% thermal ellipsoids (fluorine and hydrogen atoms omitted for clarity). Two molecules are shown. Selected bond distances (Å) and angles (°): Hg(1)−O(1) 2.877(6), Hg(2)−O(1) 2.975(6), Hg(3)−O(1) 2.846(6), Hg(2)−C(23) 3.328(10), Hg(1)−C(1) 2.071(9), Hg(1)−C(8) 2.066(9), Hg(2)−C(7) 2.071(9), Hg(2)−C(14) 2.088(9), Hg(3)−C(2) 2.065(9), Hg(3)−C(13) 2.066(8), O(1)−N(1) 1.277(9), C(8)−Hg(1)−C(1) 176.1(4), C(7)−Hg(2)−C(14) 176.4(4), C(2)−Hg(3)−C(13) 173.8(4).

Compound **3** crystallizes in the monoclinic space group *C*2/*c* (Table 1). The crystal structure of this derivative consists of isolated C_2 symmetric molecules of [**1**•NIT-Ph•**1**] in which a NIT-Ph molecule is sandwiched by two molecules of **1** (Figure 3). The two oxygen atoms of the NIT-Ph are triply coordinated to the mercury centers provided by the juxtaposed molecules of **1**. The Hg−O distances (Hg−O = 2.846(6)−2.975(6) Å) as well as the orientation of the linear N−O functionality with respect to the plane of the trinuclear mercury complex (α = 85.1°, *d* = 2.025 Å) are similar to those found in **2**. Additional interactions between **1** and NIT-Ph include two symmetrically equivalent Hg−$C_{aromatic}$ contacts of 3.33(1) Å which occur between Hg(2)/Hg(2a) and C(23)/C(23A), respectively. As in the case of **2**, neighboring molecules of [**1**•NIT-Ph•**1**] form offset $\pi-\pi$ stacking interactions (not pictured), which involve the phenylene ring containing C(7) and the phenylene ring containing C(13) in

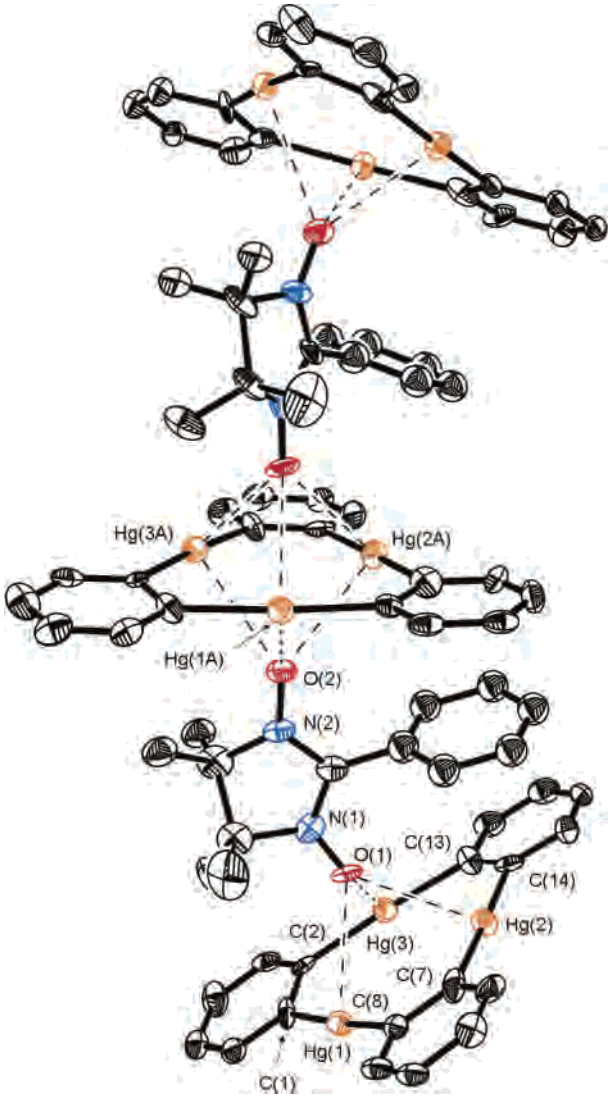

Figure 4. Portion of a polymeric chain observed in the structure of compound **4** (30% thermal ellipsoids, fluorine and hydrogen atoms omitted for clarity). Selected bond distances (Å) and angles (°): Hg(1)−O(1) 3.020(17), Hg(2)−O(1) 2.974(19), Hg(3)−O(1) 2.90(2), Hg(1A)−O(2) 2.91(2), Hg(2A)−O(2) 2.97(2), Hg(3A)−O(2) 2.99(2), Hg(1)−C(1) 2.11(3), Hg(1)−C(8) 2.08(2), Hg(2)−C(7) 2.09(3), Hg(2)−C(14) 2.12(3), Hg(3)−C(2) 2.10(2), Hg(3)−C(13) 2.09(2), O(1)−N(1) 1.28(3), O(2)−N(2) 1.27(3), C(1)−Hg(1)−C(8) 176.4(10), C(7)−Hg(2)−C(14) 177.1(9), C(2)−Hg(3)−C(13) 176.3(9).

a neighboring molecule generated by $[-x + 1, -y, -z]$ (centroid distance = 4.14 Å).

Compound **4** crystallizes in the hexagonal space group $P6_1$ (Table 1). Examination of the crystal structure reveals extended helical binary polymeric chains with alternating molecules of **1** and NIT-Ph that propagate parallel to one another (Figure 4). The interactions responsible for the formation of these infinite chains involve the triple coordination of the oxygen atoms of the NIT-Ph molecule to the mercury centers of **1**. Thus, the coordination about the molecules of **1** is similar to that encountered in [**1**•$(L)_2$] complexes. As a result, the environment of the NIT-Ph molecule as well as the coordination geometry about the NO functionalities is virtually identical to that found in **3** (α = 87.3°, d = 2.123 Å, Hg−O = 2.90(2)−3.020(17) Å). The shortest intermolecular distances between the NIT-Ph molecules involve C−H groups and not the N−O functionalities. These CH···HC distances (not pictured), in the range of 2.6−2.8 Å, occur between the phenyl and methyl groups of two NIT-Ph molecules belonging to parallel chains.

The N−O bond distance (**2**: O(1)−N(1) 1.31(2); **3**: N(1)−O(1) 1.277(9); **4**: N(1)−O(1) 1.28(3) N(2)−O(2) 1.27(3) Å) is similar to that observed in pristine TEMPO for **2** (1.29 Å)[28] and pristine NIT-Ph for **3** and **4** (1.26 and 1.27 Å).[29] The absence of significant lengthening of the N−O bonds is indicative of the weakness of the Hg−O interaction. In agreement with this view, we note that the C−Hg−C angle at each mercury atom does not substantially deviate from linearity.

To provide a better description of the interaction involving **1** and the oxygen atom of the nitroxides or nitronyl nitroxides radicals, we have studied the electronic structure of **1** using density functional theory (DFT). Examination of the literature indicates that few theoretical studies have been carried out on compound **1**. Most studies available to date were obtained using AM1,[30,31] MNDO,[32] or molecular mechanics[33] methods, and some of the results do not always agree with experimental data. For these reasons, geometry optimization and single-point energy calculations were performed using density functional theory (DFT) in the Amsterdam density functional package (ADF).[34−36] The optimized structure of **1**, which has D_{3h} symmetry, features bond distances and angles that are comparable to those determined for pure **1** by X-ray diffraction (Table 2).[37] The HOMO is largely based on the perfluorophenylene rings of **1** (Figure 5). In contrast, the LUMO bears large contributions of mercury 6p orbitals (44%) and exhibits a large lobe in the center of **1** (Figure 5). This large lobe of the LUMO located in the middle of the three mercury centers suggests that this particular region of the molecule is where Lewis acidity is at a maximum. In agreement with this view, this large lobe appears directly aligned with the direction along which Lewis basic substrates, including TEMPO and NIT-Ph, bind to the molecule. These results lend support to the claim that the Lewis acidic character of **1** is dominated by the empty 6p orbitals on the mercury. However, the computed magnitude of the HOMO−LUMO gap, which is equal to 3.357 eV, indicates that the

(28) Bordeaux, D.; Lajzerowicz-Bonneteau, J.; Briere, R.; Lemaire, H.; Rassat, A. *Org. Magn. Reson.* **1973**, *5*, 47−52.
(29) Zheludev, A.; Barone, V.; Bonnet, M.; Delley, B.; Grand, A.; Ressouche, E.; Rey, P.; Subra, R.; Schweizer, J. *J. Am. Chem. Soc.* **1994**, *116*, 2019−2027.
(30) Chistyakov, A. L.; Stankevich, I. V.; Gambaryan, N. P.; Struchkov, Yu. T.; Yanovsky, A. I.; Tikhonova, I. A.; Shur, V. B. *J. Organomet. Chem.* **1997**, *536*, 413−424.
(31) Castro, E. A. *Molecules* **2003**, *8*, 418−429.
(32) Saitkulova, L. N.; Bakhmutova, E. V.; Shubina, E. S.; Tikhonova, I. A.; Furin, G. G.; Bakhmutov, V. I.; Gambaryan, N. P.; Chistyakov, A. L.; Stankevich, I. V.; Shur, V. B.; Epstein, L. M. *J. Organomet. Chem.* **1999**, *585*, 201−210.
(33) Castro, E. A. *J. Mol. Struct. (THEOCHEM)* **2002**, *619*, 45−50.
(34) ADF2003.01. SCM, Theoretical Chemistry, Vrije Universiteit, Amsterdam, The Netherlands.
(35) Guerra, C. F.; Snijders, J. G.; Te Velde, G.; Baerends, E. *J. Theor. Chem. Acc.* **1998**, *99*, 391−403.
(36) Te Velde, G.; Bickelhaupt, F. M.; Baerends, E. J.; Fonseca Guerra, C.; Van Gisbergen, S. J. A.; Snijders, J. G.; Ziegler, T. *J. Comput. Chem.* **2001**, *22*, 931−967.
(37) Haneline, M. R.; Gabbaï, F. P. *Z. Naturforsch.* **2004**, *59B*, 1483−1487.

Table 1. Crystal Data, Data Collection, and Structure Refinement for **2**, **3**, and **4**

	2	**3**	**4**
		Crystal Data	
formula	$C_{27}H_{18}F_{12}Hg_3NO$	$C_{49}H_{17}F_{24}Hg_6N_2O_2$	$C_{31}H_{17}F_{12}Hg_3N_2O_2$
M_r	1202.19	2325.19	1279.24
crystal size (mm^3)	0.36 × 0.18 × 0.06	0.44 × 0.41 × 0.32	0.34 × 0.28 × 0.22
crystal system	triclinic	monoclinic	hexagonal
space group	*P*1	*C*2/c	*P*6(1)
a (Å)	10.263(2)	17.963(4)	11.559(3)
b (Å)	12.009(2)	15.835(3)	11.559(3)
c (Å)	12.669(3)	20.652(4)	44.627(14)
α (°)	87.16(3)		
β (°)	70.83(3)	115.67(3)	
γ (°)	74.77(3)		
V ($Å^3$)	1421.9(5)	5294.8(18)	5164(2)
Z	2	4	6
ρ_{calc} (g cm^{-3})	2.808	2.917	2.468
μ(Mo Kα) (mm^{-1})	16.259	17.460	13.441
F(000) (e)	1086	4148	3486
		Data Collection	
T/K	110(2)	110(2)	110(2)
scan mode	w	w	w
hkl range	−11→11, −13→13, −14→14	−21→21, −18→16, −24→24	−12→12, −12→12, −49→47
measured reflns	8204	19319	32596
unique reflns [R_{int}]	3989 [0.0404]	4659 [0.0386]	4893 [0.0737]
reflns used for refinement	3989	4659	4893
abs correction	SADABS	SADABS	Empirical
T_{min}/T_{max}	0.266545	0.313625	0.352/0.827
		Refinement	
refined params	361	376	397
R1,[a] wR2[b] [$I > 2\sigma(I)$]	0.0596, 0.1329	0.0272, 0.0643	0.0478, 0.1215
ρ_{fin} (max/min) (e $Å^{-3}$)	3.906, −3.468	1.001, −0.988	2.348, −1.302

[a] $R1 = \Sigma(F_o - F_c)/\Sigma F_o$. [b] $wR2 = \{[\Sigma w(F_o^2 - F_c^2)^2]/[\Sigma w(F_o^2)^2]\}^{1/2}$; $w = 1/[\sigma^2(F_o^2) + (ap)^2 + bp]$; $p = (F_o^2 + 2F_c^2)/3$; $a = 0.02$ (**2**), 0.0485 (**3**), 0.07 (**4**); $b = 100$ (**2**), 0 (**3**), 80 (**4**).

Table 2. Experimental and Calculated Bond Distances (Å) and Angles (°) for the Structure of **1**

	(1) DFT	**1** (X-ray)[a]	Optimized geometry of **1** and numbering scheme
Hg(1)-C(3)	2.132	2.072	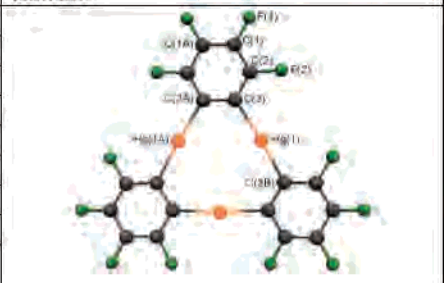
C(1)-C(1A)	1.396	1.389	
C(1)-C(2)	1.396	1.381	
C(1)-F(1)	1.353	1.342	
C(2)-C(3)	1.391	1.376	
C(2)-F(2)	1.369	1.357	
C(3)-C(3A)	1.418	1.416	
Hg(1)-Hg(1A)	3.694	3.610	
C(3)-Hg(1)-C(3B)	175.2	175.3	

[a] Average metrical parameters derived from the crystal structures of four polymorphs of **1**.[37]

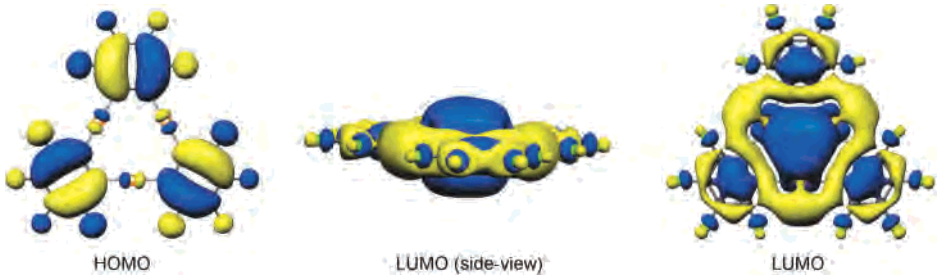

Figure 5. Views of the HOMO and LUMO of compound **1**.

LUMO might be too high in energy to efficiently mix with the donor orbitals of the ligand. This conclusion is also supported by the cyclic voltammogram of **1** in THF using $^nBu_4PF_6$ as a supporting electrolyte which does not show any reduction in the solvent window. As a result, the bonding in adducts such as **2**, **3**, and **4** is most likely dominated by electrostatic rather than covalent interactions. This conclusion is in agreement with the work of Fackler[38] who showed, by

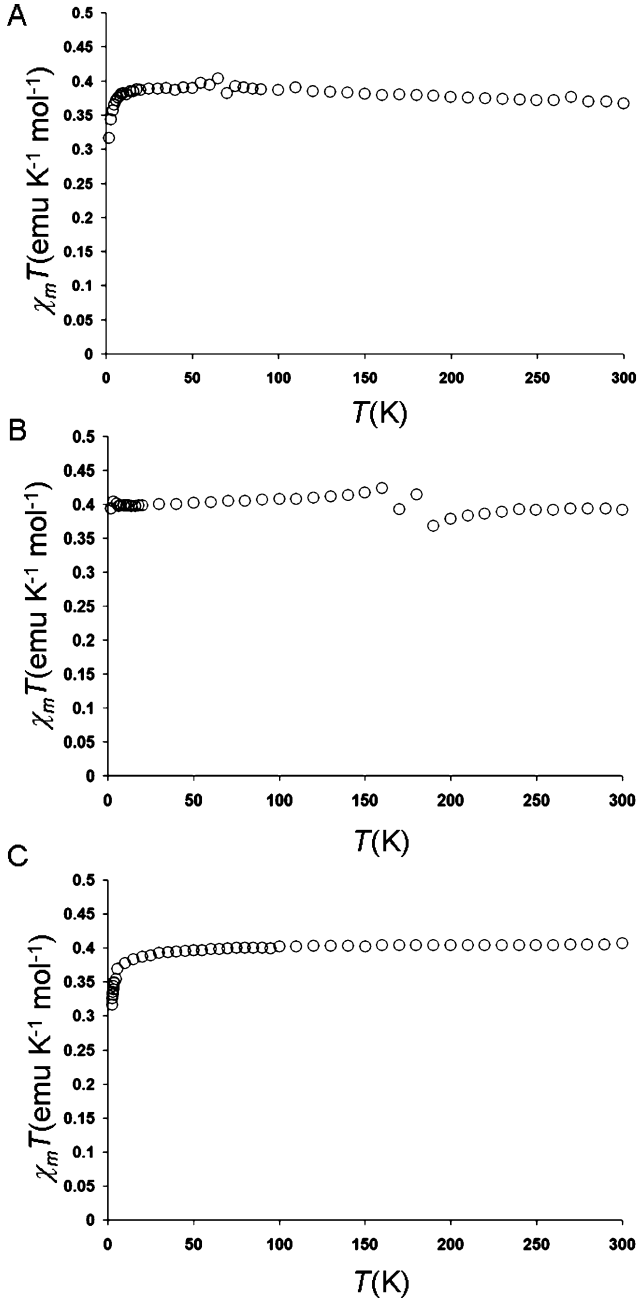

Figure 6. Thermal variation of the X_mT product for compound **2** (A), compound **3** (B), and compound **4** (C) in the 2−300 K range.

a single-point energy DFT calculation, that the electrostatic potential surface at the center of the trinuclear macrocycle is positive while the periphery is negative.

Variable-temperature (2−300 K) magnetic susceptibility data were collected on crushed single crystals of compounds **2**−**4** (Figure 6). In all three cases the room temperature X_mT (0.4 emu K mol^{-1}) is in good agreement with the expected value for an isolated molecule with one unpaired electron ($S = {}^1/_2$). In the case of **3,** which contains isolated sandwiches of [**1**•NIT-Ph•**1**], the X_mT remains constant over the entire temperature range, indicating the absence of detectable magnetic interactions. This observation appears to be in agreement with the large separation of the spin-bearing NIT-Ph molecules which do not form intermolecular contacts below 4.8 Å. It also indicates that the molecules of **1** act as efficient magnetic insulators. It is important to note that the behavior of [**1**•NIT-Ph•**1**] parallels that of solid [**1**•Cp-NiCp•**1**] in which the sandwiched nickelocene molecules appear insulated from one another.[39] In the case of **2** and **4**, X_mT remains independent of temperature until approximately 10 K, at which point a sharp decrease is observed, indicating probable long-range anti-ferromagnetic coupling. The Weiss constant for **2** ($\theta = -0.17$ K) is in agreement with this extremely weak coupling. In the case of **4**, the Weiss constant ($\theta = -1.41$ K) is, in fact, similar to that observed for pristine NIT-Ph.[40] Because of the weakness of these antiferromagnetic interactions, a definitive assignment of the coupling pathways cannot be unequivocally established. In the case of **2**, these weak interactions possibly result from intermolecular interactions between proximal TEMPO molecules (Figure 2). In the case of **4**, the weak anti-ferromagnetic interactions could be mediated by the trinuclear mercury complex. However, the observed orientation places the SOMO of the NIT-Ph molecule, which has π-symmetry,[41] almost orthogonal to the LUMO of **1**. As a result, the mediation of magnetic interactions by the trinuclear mercury complex can only be minimal. Hence, the presence of short intermolecular distances between NIT-Ph molecules belonging to parallel chains as discussed above could also be associated with this weak magnetic interaction.

Concluding Remarks

We have demonstrated that **1** forms adducts with organic nitronyl radicals where the electron-rich terminus of the N−O moiety interacts with the three mercury centers of **1**. The structure of adducts **2**−**4** is reminiscent of that observed for other adducts involving **1** and donors such as organic carbonyls,[8−10] nitriles,[11] and sulfoxides.[12] The DFT calculations that we have performed suggest that the LUMO of **1** might be too high in energy to significantly interact with filled orbitals of the donors. In turn, these investigations suggest that the interaction between **1** and the radical is mostly electrostatic rather than covalent. A similar conclusion can be extended to adducts of **1** with other donors including organic carbonyls, nitriles, and sulfoxides.[3,4,6,8−12] Finally, **1** does not appear to mediate effective magnetic coupling of nitronyl nitroxides coordinated on either side of its molecular plane. The high energy of the unoccupied orbitals of **1** as well as the perpendicular orientation of the nitronyl nitroxide ring with respect to the plane of the trinuclear complex are most likely responsible for the absence of significant coupling. Altogether, these results suggest that **1** may serve to insulate molecules with unpaired electrons. The properties of [**1**•NIT-Ph•**1**], which do not show any magnetic coupling, certainly corroborate this view. To further support this

(38) Burini, A.; Fackler, J. P., Jr.; Galassi, R.; Grant, T. A.; Omary, M. A.; Rawashdeh-Omary, M. A.; Pietroni, B. R.; Staples, R. J. *J. Am. Chem. Soc.* **2000**, *122*, 11264−11265.

(39) Haneline, M. R.; Gabbaï, F. P. *Angew. Chem., Int. Ed.* **2004**, *43*, 5471−5474.

(40) Awaga, K.; Maruyama, Y. *J. Chem. Phys.* **1989**, *91*, 2743−2747.

(41) D'Anna, J. A.; Wharton, J. H. *J. Chem. Phys.* **1970**, *53*, 4047−52.

argument, we are currently focusing on the synthesis of complexes in which the mercury centers of **1** are directly facing the SOMO of π-delocalized radicals.

Acknowledgment. We would like to thank Curtis Berlinguette, Eric Schelter, and Professor Kim Dunbar for their assistance with the magnetic measurements and discussions; James Gardinier for the synthesis of NIT-Ph; Tim Hugbanks and Lindsay Roy for their help with the ADF calculations. Acknowledgment is made to the donors of the American Chemical Society Petroleum Research Fund for support of this research (Grant ACS PRF# 38143 -AC 3). M.R.H. thanks Proctor and Gamble for a graduate fellowship.

Supporting Information Available: X-ray crystallographic data for **2**, **3,** and **4** in CIF format. This material is available free of charge via the Internet at http://pubs.acs.org.

IC050528A